Development and Evaluation of a Multi-Modal Hyaluronic Acid Hydrogel for Anti-Inflammatory Drug Delivery for Multiple Sclerosis Therapy

Tutut Ummul Habibah, Ph.D.

Doctoral Thesis Summary

Tomas Bata University in Zlín

Tomas Bata University in Zlín
Faculty of Technology

Doctoral Thesis Summary

Development and Evaluation of a Multi-Modal Hyaluronic Acid Hydrogel for Anti-Inflammatory Drug Delivery for Multiple Sclerosis Therapy

Vývoj a charakterizace multimodálního hydrogelu kyseliny hyaluronové s řízeným uvolňováním protizánětlivých léčiv k léčbě roztroušené sklerózy

Author: **Tutut Ummul Habibah, Ph.D.**

Degree programme: Technology of Macromolecular Substance
P0531D130058

Supervisor: doc. RNDr. Marek Ingr, Ph.D.
PharmDr. Martin Pravda, Ph.D. (Contipro)

External examiners: Ing. František Ondreáš, Ph.D.
Prof. RNDr. Miroslav Štěpánek, Ph.D.

Zlín, August 2025

Published by **Tomas Bata University in Zlín** in the Edition **Doctoral Thesis Summary.**
The publication was issued in the year 2025

Klíčová slova*: Řízené uvolňování léčiv, hyaluronová kyselina, chondroitin sulfát, hydrogely, zánět, minocyklin, roztroušená skleróza, komplexy polyelektrolytů, syntetický preimplantační faktor*

Key words: *Controlled Drug Delivery Systems, Hyaluronic acid, Chondroitin Sulphate, Hydrogels, Inflammatory, Minocycline, Multiple Sclerosis, Polyelectrolyte Complexes, Synthetic Pre-Implantation Factor*

Full text of the doctoral thesis is available in the Library of TBU in Zlín.

ISBN 978-80-7678-351-5

ABSTRACT

Current treatments for multiple sclerosis (MS) are hindered by adherence challenges linked to frequent systemic dosing regimens, which demand active patient participation and often lead to suboptimal therapeutic outcomes. Conventional disease-modifying therapies (DMTs) administered orally or via injection, struggle to balance efficacy with patient quality of life, compounded by risks of systemic toxicity and rapid drug clearance. Recent surveys underscore a growing demand for implantable drug delivery systems (DDS) that minimize dosing frequency, reduce patient burden, and enhance long-term compliance.

This dissertation addresses these unmet needs by developing an injectable hydrogel platform based on aldehyde-functionalized hyaluronic acid (HAOX) and chondroitin sulfate (CSOX), designed for localized, sustained delivery of anti-inflammatory therapeutics. Central to this innovation is the immobilization of polyelectrolyte complexes (PECs) within the covalently crosslinked hydrogel matrix. Unlike conventional nanoparticle-based DDS, which rely on freely diffusing carriers prone to burst release and instability, immobilized PECs exploit electrostatic interactions between therapeutic agents (minocycline, MN; Fluorescein isothiocyanate-modified synthetic Preimplantation Factor, FITC-SPIF) and the anionic sulfate groups of CSOX. This strategy enhances drug retention, reduces manufacturing complexity, and eliminates the need for costly encapsulation processes.

For MN, a repurposed tetracycline antibiotic, PECs formed with Ca^{2+} and gelatin achieved sustained release over 288 hours with an 88% reduction in burst release compared to unbound formulations. Similarly, FITC-SPIF, an immunomodulatory peptide, exhibited prolonged delivery kinetics proportional to CSOX concentration, minimizing premature leakage. The hydrogel's enzymatic resistance, injectability (<185 kPa extrusion force, Dynamic Glide Force < 40 N), and mechanical adaptability (storage modulus: 125–1,083 Pa) ensure structural stability under physiological conditions, addressing key limitations of prior DDS.

In vitro validation confirmed therapeutic bioactivity: released MN suppressed pro-inflammatory IL-6 secretion by 56% in human monocytes, while FITC-SPIF promoted TGF-β expression in macrophages, indicative of anti-inflammatory polarization. By integrating immobilized PECs with a tuneable HAOX-CSOX matrix, this platform resolves the historical trade-offs between controlled release, scalability, and clinical practicality.

This work advances MS therapy by offering a patient-centric solution that aligns with preferences for minimally invasive and long-acting treatments. The

HAOX-CSOX hydrogel's cost-effective design, coupled with its capacity to deliver diverse therapeutics, positions it as an alternative tool for managing chronic neuroinflammatory diseases, bridging the gap between material innovation and patient-centred care.

ABSTRAKT

Současné terapie roztroušené sklerózy (RS) jsou limitovány problémy s dodržováním léčebných režimů založených na častém dávkování léčiv, které vyžadují aktivní účast pacientů, což vede ke snížené terapeutické účinnosti. Terapie modifikující onemocnění (DMTs), podávaná perorálně nebo injekčně, nedokáže účinně sladit klinický přínos s kvalitou života pacientů, a to zejména v důsledku systémové toxicity a rychlé eliminace léčiv. Nedávné průzkumy zdůrazňují rostoucí poptávku po implantovatelných systémech pro řízené uvolňování léčiv (DDS), které minimalizují frekvenci aplikace, snižují zátěž pacientů a zlepšují dlouhodobou adherenci.

Tato disertační práce řeší tyto nedostatky vývojem injekčně aplikovatelného hydrogelového systému na bázi aldehydem modifikované hyaluronové kyseliny (HAOX) a chondroitin sulfátu (CSOX), určeného pro lokalizované a prodloužené uvolňování protizánětlivých léčiv. Klíčovou inovací je imobilizace polyelektrolytových komplexů (PECs) v kovalentně zesíťované hydrogelové matrici. Na rozdíl od konvenčních DDS založených na nanočásticích, které využívají volně difundující nosiče náchylné k prvotnímu prudkému uvolnění (burst effect) a nestabilitě, imobilizované PECs využívají elektrostatické interakce mezi terapeutiky (minocyklin, MN; fluoresceinisothiokyanátem modifikovaný syntetický preimplantační faktor, FITC-SPIF) a aniontovými sulfátovými skupinami CSOX. Tato strategie zvyšuje retenci léčiv, snižuje výrobní náročnost a eliminuje potřebu nákladných enkapsulačních procesů.

Pro MN, repurposed antibiotikum ze skupiny tetracyklinů, dosáhly PECs s Ca^{2+} a želatinou prodlouženého uvolňování po dobu 288 hodin s 88% redukcí prudkého uvolňování ve srovnání s neimobilizovanými formami. Podobně FITC-SPIF, imunomodulační peptid, vykazoval kinetiku uvolňování úměrnou koncentraci CSOX, což minimalizovalo předčasnou ztrátu účinné látky. Enzymatická odolnost hydrogelu, injekční aplikovatelnost (<185 kPa vytlačovací síla, dynamická kluzná síla <40 N) a mechanická adaptabilita (elastická složka dynamického modulu ve smyku G‘: 125–1 083 Pa) zajišťují strukturální stabilitu za fyziologických podmínek, čímž řeší hlavní omezení předchozích DDS.

In vitro testy potvrdily biologickou aktivitu uvolňovaných léčiv a kompatibilitu systému HAOX-CSOX: uvolněný MN potlačil sekreci prozánětlivého IL-6 v lidských monocytech o 56 %, zatímco FITC-SPIF

indukoval expresi TGF-β v makrofázích, což indikuje protizánětlivou polarizaci. Integrací imobilizovaných PECs do matrice HAOX-CSOX tato platforma překonává tradiční kompromisy mezi řízeným uvolňováním, škálovatelností a klinickou praktičností.

Práce přináší inovativní řešení pro léčbu RS, které odpovídá preferencím pacientů pro minimálně invazivní a dlouhodobě působící terapie. Nákladově efektivní design hydrogelu HAOX-CSOX spolu s jeho schopností dodávat různé terapeutické látky jej předurčuje jako alternativní nástroj pro léčbu chronických neurozánětlivých onemocnění, propojující materiálový výzkum s potřebami pacientů.

Table of Contents

ABSTRACT 3

ABSTRAKT 5

1. INTRODUCTION AND CURRENT STATE OF THE ART OF THE ISSUE DEALT WITH 9

1.1 INTRODUCTION 9
1.2 CURRENT STATE OF THE ART 9
1.2.1 PATHOETIOLOGY OF MULTIPLE SCLEROSIS 9
1.2.2 SYSTEMIC TOXICITY OF CONVENTIONAL MS TREATMENT: A HIDDEN COST OF CONVENTIONAL DELIVERY 10
1.2.3 SOCIOECONOMIC IMPLICATION OF CONVENTIONAL MULTIPLE SCLEROSIS TREATMENT AND POTENTIAL TREATMENT STRATEGY 11
1.2.4 MINOCYCLINE: FROM ANTIBIOTIC TO NEUROPROTECTANT 11
1.2.5 FROM GESTATION TO NEUROPROTECTION: REPURPOSING SYNTHETIC PREIMPLANTATION FACTOR FOR IMMUNOMODULATION IN MULTIPLE SCLEROSIS 12
1.2.6 HYDROGELS: PROMISES AND PITFALLS 12
1.2.7 POLYELECTROLYTE COMPLEXES (PEC): SCALABILITY VERSUS STABILITY 13
1.2.8 TOWARD A PARADIGM SHIFT: THE HAOX-CSOX HYDROGEL PLATFORM 13

2. AIM OF THE THESES 13

3. EXPERIMENTAL SECTIONS 15

3.1 MATERIALS AND SYNTHESIS 15
3.1.1 HYDROGEL FORMULATIONS 15
3.2 CHARACTERIZATION TECHNIQUES 18
3.2.1 GELATION TIME 18
3.2.2 SWELLING RATIO (Q) 19
3.2.3 DRUG RELEASE EXPERIMENT 19
3.2.4 INJECTABILITY 20
3.2.5 BIOACTIVITY ASSAYS 20
3.3 DATA PROCESSING AND STATISTICAL APPROACHES 20

4. RESULT AND DISCUSSION 21

4.1 IN SITU INJECTABLE HYALURONIC ACID HYDROGEL LOADED WITH POLYELECTROLYTE COMPLEX FOR MINOCYCLINE CONTROL RELEASE 21
4.1.1 SYNTHESIS OF ALDEHYDE-MODIFIED CHONDROITIN SULFATE (CSOX) 21
4.1.2 GELATION DURATION AND INJECTABILITY OF HAOX-BASED DDS 22

4.1.3 Minocycline release profiles and the mechanism in injectable HAOX-based drug delivery system 23
4.1.4 The influence of swelling behaviour on sustained MN release in hydrogel-based delivery system 24
4.2 In situ forming hydrogel from aldehyde-modified hyaluronic acid and aldehyde-modified chondroitin sulfate for synthetic preimplantation factor delivery 25
4.2.1 Gelation time of FITC-SPIF-loaded HAOX-CSOX hydrogels: balancing pH-dependent crosslinking for clinical translation 25
4.2.2 Release study of FITC-SPIF, T50 %, and Korsmeyer-Peppas parameters 26
4.2.3 Swelling profile and crosslinking density of the drug delivery system 27
4.2.4 Injectability of the drug delivery system 28
4.2.5 FITC-SPIF-induced macrophage polarization: an in vitro bioactivity study 28

5. CONCLUSIONS 29

REFERENCES 31

LIST OF FIGURES 34

LIST OF TABLES 35

LIST OF ABBREVIATIONS 36

CURRICULUM VITAE 38

LIST OF PUBLICATION 39

OVERVIEW OF OTHER ACTIVITIES 39

1. INTRODUCTION AND CURRENT STATE OF THE ART OF THE ISSUE DEALT WITH

1.1 Introduction

Multiple sclerosis (MS) is an autoimmune-driven neuroinflammation and demyelination of central nervous system (CNS) contributing to escalating motor, sensory, and cognitive deficits. Current Disease-Modifying Therapies (DMTs), slow disease progression but face limitations in administrations, including high cost, patient burden, and non-compliance. Autoinjectors and oromucosal sprays improves self-administration yet need daily replenishment, creating burdensome regimens. Recent surveys report growing patient preference for implantable drug delivery systems (DDS) that provide sustained DMTs release with minimal patient intervention.

This study proposes an injectable DDS based on an aldehyde-modified hyaluronic acid hydrogel (HAOX) integrated with immobilized polyelectrolyte complexes (PEC) composed of aldehyde-modified chondroitin sulfate (CSOX). This system addresses burst release and stability challenges in hydrogel DDS by tuning release profile via PEC incorporation. It delivers two repurposed therapeutics:

- Minocycline (MN), an affordable tetracycline antibiotic with neuroprotective properties.
- Fluorescein isothiocyanate–modified Synthetic Preimplantation Factor (FITC-SPIF): A peptide with potent immunomodulatory effects.

The HAOX hydrogel ensures structural integrity for injection and localization, enhancing drug concentration while minimizing systemic toxicity. This approach simplifies administration, reduces cost and dosing frequency, and eliminates dependency on patient involvement. The research is structured in two phases to investigate HAOX-CSOX's structural properties and release mechanism for MN and FITC-SPIF.

1.2 Current state of the art

1.2.1 Pathoetiology of multiple sclerosis

MS is as a progressive inflammatory degenerative disease of the CNS driven by interdependent pathobiological axes. The inflammation dysregulates cytokines (IL-6, TGF-β, TNF-α, IFN-γ), disrupting the blood-brain barrier (BBB) and

promoting T and B cells migration and pro-inflammatory macrophage polarization, leading to demyelination [1,2].

Food and Drug Administration (FDA) - approved DMTs (Table 1.1) vary in administration routes and frequency.

- Daily: Teriflunomide (oral), Glatiramer acetate (injection).
- Infusions: Ocrelizumab (every 6 months), Natalizumab (every 4 weeks) [3].

DMTs reduce relapse frequency by 30-50%, but adherence is compromised by needle anxiety, injection-site reactions, and cognitive/motor impairments. Adherence reduced from 69.4% (weekly intramuscular) to 58.4% (thrice-weekly subcutaneous) [4,5].

Table 1.1 FDA Approved Disease Modifying Therapies [3,6–8].

DMTs	**Route of administration**	**Approved indication**	**Mechanism of action**
Interferon beta 1a	Injection	Clinically Isolated Syndrome (CIS); Relapsing Remitting MS (RRMS)	Immunomodulatory
Interferon beta 1b	Injection	CIS; RRMS	Immunomodulatory
Ocrelizumab	Infusion	CIS; RRMS; Active SPMS; Primary Progressive MS (PPMS)	Depletion of CD20+ cells
[*Full table in original document*]			

1.2.2 Systemic toxicity of conventional MS treatment: a hidden cost of conventional delivery

Systemic DMT administration distributes drugs to healthy and diseased tissues (Fig. 1.2), requiring supratherapeutic doses that risk toxicity:

- Interferon Beta-1: 60% of patients experience nausea; 10-15% report hepatotoxicity [9,10].
- Dimethyl fumarate: High-oral doses (240 mg twice daily) cause lymphopenia in 15-20% of patients due to low CSF concentrations (1 µg mL^{-1} vs. neuroprotective threshold of 30-50 µg mL^{-1}) [9,11].
- Ocrelizumab: Increase susceptibility to respiratory infections [12].

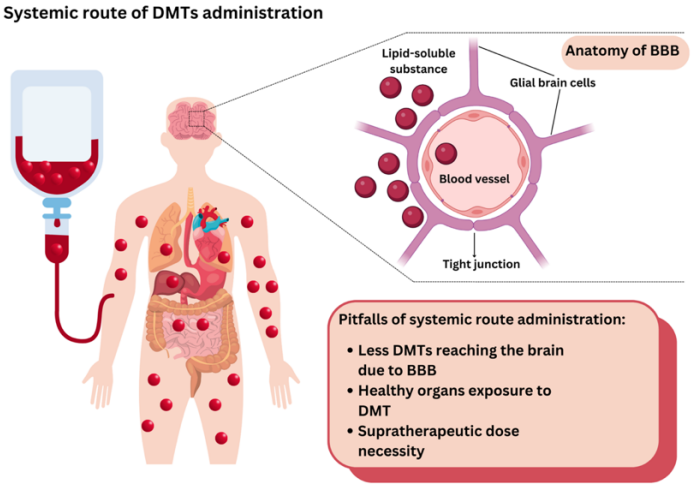

Fig. 1.1: Risk of systemic administration route of the Disease Modifying Therapies.

Adverse effects incur hidden costs, including management of infusion-related hypersensitivity (affecting 25% of patients) and socioeconomic burdens from lost income/caregiving [13,14].

1.2.3 Socioeconomic implication of conventional multiple sclerosis treatment and potential treatment strategy

Annual DMT cost rose from $26,772 (2011) to $43,606 (2015), straining healthcare systems and patients [15]. MS disproportionately affects women (3:1 female-to-male prevalence ratio, causing workforce attrition and a severe decline in living standards [16]. Drug repurposing offers a cost-effective strategy by leveraging existing drugs:

- Accelerates development, bypassing early-stage testing [17].
- Candidates like MN (neuroprotective) and SPIF (immunomodulation) target MS pathophysiology.

1.2.4 Minocycline: from antibiotic to neuroprotectant

MN is repurposed for MS due to:

- Low cost ($0.50/day vs. $6,000/month for monoclonal antibodies) [18,19].

- Dual mechanisms: Microglial depletion and BBB stabilization via ZO-1, Occludin maintenance [20,21].
- Limitations: Narrow therapeutic window. Neuroprotection requires high doses (100-200 mg/day), causing hepatotoxicity [22] and mortality in animal studies [23]. CSF concentrations (0.5 µg/mL) remain suboptimal [24,25].
- Delivery challenges: pH-dependent solubility, cation chelation cations (Ca^{2+}, Fe^{3+}) and instability in acidic environments (Fig. 1.2) [26,27].

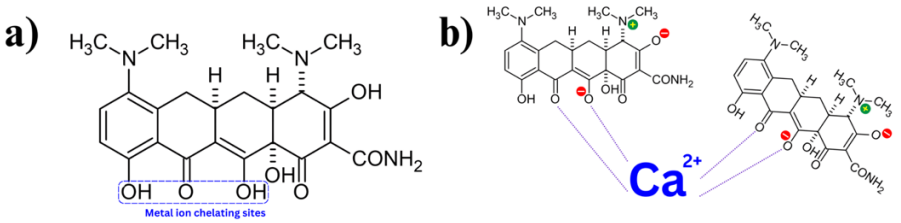

Fig. 1.2: Minocycline structure: a) metal ion chelation sites, b) chelation structure of MN with Calcium (Holmkvist et al., 2016; Z. Zhang et al., 2015).

1.2.5 From gestation to neuroprotection: repurposing synthetic preimplantation factor for immunomodulation in multiple sclerosis

SPIF (MVRIKPGSANKPSDD; Fig. 1.3) is a 15-amino acid peptide with fast-track clinical potential [28]. It:

- Suppresses pro-inflammatory cytokines (IL-6 and IFN-γ) and promotes TGF-β expression, while harnessing the ability to cross the BBB [29,30].
- Limitations: Rapid enzymatic degradation (<2 h half-life) and limited brain uptake (5% of dose) [30].

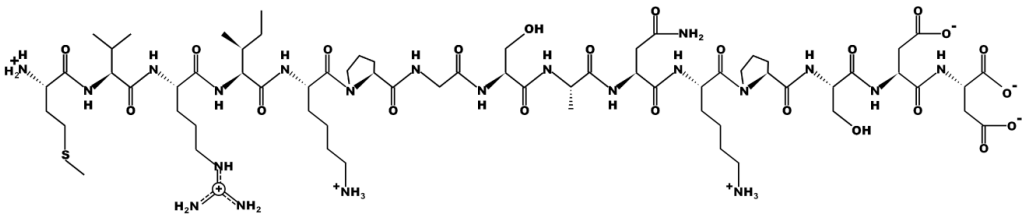

Fig. 1.3: Structure of synthetic preimplantation (SPIF).

1.2.6 Hydrogels: promises and pitfalls

Hydrogels offer biocompatibility, tuneable mechanics, and localized release but face significant challenges. A persistent limitation is burst release, exemplified by Poloxamer 407 system releasing 50% of MN within 24 h [31,32]. Similarly, HA/CS hydrogels degrade rapidly in inflammatory environments rich

in hyaluronidases and chondroitinase, causing premature drug leakage [33]. While strategies like PLGA nanoparticles encapsulating MN-Ca^{2+} chelates prolong release, they introduce scalability barriers due to inflammatory risks from acidic degradation byproducts [34].

1.2.7 Polyelectrolyte complexes (PEC): scalability versus stability

PECs form self-assembled networks via electrostatic interactions, simplifying manufacturing by omitting organic solvents [35]. However, MN's zwitterionic nature (isoelectric point: 6.4) limits complex stability, yielding ≤ 30% entrapment efficiency [36]. Physiological fluctuations in pH and ionic strength further disrupt electrostatic conformations, accelerating drug leakage [35]. Scalability is hindered by batch inconsistencies in natural polymers (e.g., chitosan, CS) and cytotoxicity risks from synthetic alternatives like polyethylenimine [37,38].

1.2.8 Toward a paradigm shift: the HAOX-CSOX hydrogel platform

The HAOX-CSOX platform addresses these limitations through regioselective oxidation, forming covalent oxime bonds with O,O′-1,3-propanediylbishydroxylamine dihydrochloride (PDHA) to enhance hydrolytic stability [39–41]. Its dual crosslinking system, combining covalent oxime bonds and electrostatic PEC interactions, potentially minimizes burst release. The hydrogel resists enzymatic degradation by hyaluronidases/chondroitinase, enabling predictable release modelled via Korsmeyer-Peppas kinetics [42,43]. Biocompatibility studies confirm no cytotoxicity in fibroblasts [39–41,44].

2. AIM OF THE THESES

This study is aimed to develop an injectable HAOX-CSOX hydrogel platform for localized, sustained drug delivery in MS, addressing the adherence burden and pharmacokinetic limitations of current DMTs. We hypothesize that:

1. Covalent immobilization of PECs within the hydrogel network via oxime ligation will minimize burst release and prolong therapeutic delivery by restricting drug diffusion, compared to conventional freely diffusing carriers.
2. Tuning HAOX:CSOX ratios would enable precise control over hydrogel mechanical properties (e.g., gelation time, elastic modulus) and drug release kinetics, balancing injectability with structural stability.

Specifically, this thesis focusses on designing, fabricating, and analysing PEC-loaded HAOX-CSOX DDS for controlled release of anti-inflammatory drugs (Fig. 2.1). Two strategies are used:

1. Designing a MN-loaded system leveraging electrostatic PEC formation (MN/Ca^{2+}/gelatine/CSOX) and covalent HAOX-CSOX crosslinking to protect MN from degradation while ensuring sustained anti-inflammatory release.
2. Engineering a FITC-SPIF delivery platform using HAOX-CSOX double networks to optimize peptide release profiles and validate retained bioactivity post-encapsulation.

By prioritizing patient-centric design through minimally invasive administration, reduced dosing frequency, and localized delivery, this work seeks to advance a translatable alternative to systemic DMTs, bridging material innovation with clinical pragmatism.

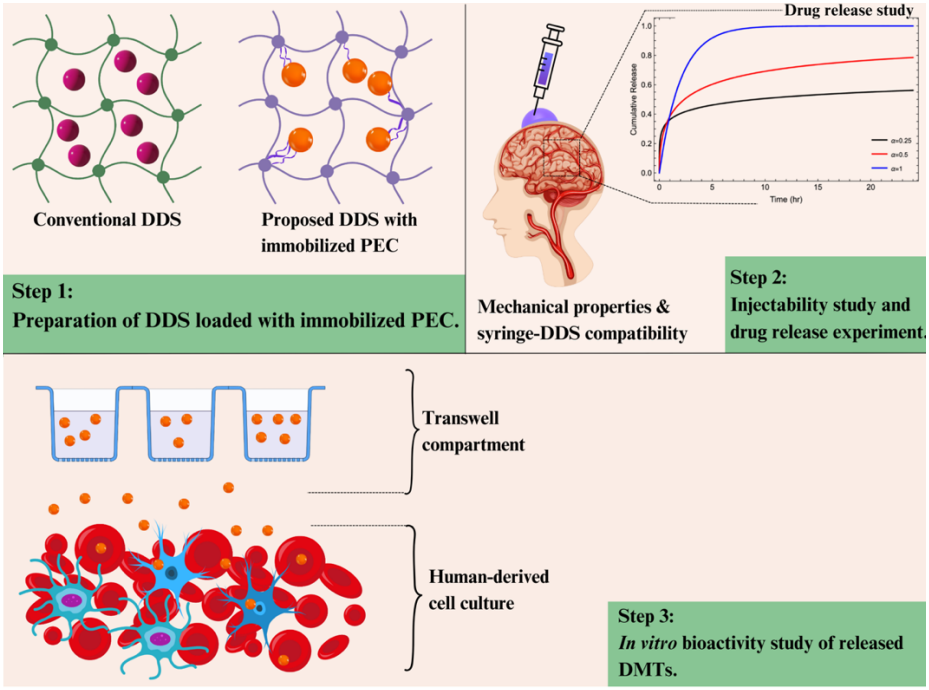

Fig. 2.1: Overview of the thesis objectives. Step 1) Materials selection and entrapment strategy for delivering repurposed DMTs. The purple sphere represents the conventional nanoparticle-based drug entrapment approach, while the orange sphere illustrates the proposed method, where the drug is encapsulated in a PEC immobilized withing the HAOX-CSOX hydrogel structure. Step 2) Characterization of DDS. Step 3) In vitro bioactivity testing to evaluate the compatibility of the DDS with the encapsulated DMTs.

3. EXPERIMENTAL SECTIONS

3.1 Materials and synthesis

Aldehyde-modified hyaluronic acid (HAOX; Molecular weight: 325 kDa; degree of substitution: 7.1%) and aldehyde-modified chondroitin sulfate (CSOX) are served as primary polymers. CSOX was synthesized via one-pot oxidation of bovine CS (Bioiberica) using 4-AcNH-TEMPO/NaClO, purified by dyalisis (14 kDa MWCO) and lyophilized. The degree of functionalization (DF) was quantified via ^{1}H NMR (Bruker Avancr Neo 700 MHz) using equation 3.1, while SEC-MALLS characterized molecularnmass. Minocycline hydrochloride (Merck) and FITC-SPIF peptide (Iris Biotech) were the therapeutic agents.

$$\mathrm{DF} = \frac{\mathrm{I}_{-\mathrm{CHO}}}{\mathrm{I}_{-\mathrm{CH_3}}} \times 300\% \qquad (3.1)$$

$\mathrm{I}_{-\mathrm{CHO}}$ indicates the integrated signal at either 9.217 ppm or 6.296 ppm, attributed to -CHO of the modified N-acetylgalactosamine unit (GalNAc). Meanwhile, $\mathrm{I}_{-\mathrm{CH_3}}$ corresponds to the integral of the signal at 2.02 ppm, for -CH_3 of GalNAc. The factor of 300 in the DF calculation accounts for both the proton ration correction and percentage conversion.

3.1.1 Hydrogel formulations

Hydrogels-based DDS were prepared using a system consisting of syringe pair with luer connection (Fig. 3.1) for covalent crosslinking between HAOX/CSOX and PDHA. Formulations (Tables 3.1 for Minocycline DDS, and Table 3.2-3.4 for FITC-SPIF DDS) included:

- **MN systems**: HAOX_MN (HAOX + MN), HAOX_CHELATE (HAOX + MN-Ca^{2+}), HAOX_PECS (unbound PEC: HAOX + MN-Ca^{2+} - gelatine-CS), HAOX_PECOX (immobilized PEC: HAOX + MN-Ca^{2+} - gelatine-CSOX).

- **FITC-SPIF systems**: HAOX_1**X** (DDS containing only 2% (w/v) HAOX, **X** signifies preparation pH, whether the formulation prepared at pH 5 or 6.8 rounded to 7). **HACOX_2X** (DDS containing 1% HAOX and 0.5% CSOX, prepared at pH **X**). **HACOX_3X** (containing 1% HAOX and 1% CSOX, prepared at pH **X**), **HACOX_37_YYY** (containing 1% HAOX and 1% CSOX, prepared at pH **6.8**, with **YYY µg** of FITC_SPIF), **HACOX_Z7_250** (DDS prepared with 1% HAOX. "**Z**" represents the concentration of CSOX, formulated at pH **6.8**, and containing **250 µg** of FITC_SPIF).

PDHA concentrations were calculated stoichiometrically (Equations 3.2 – 3.3) to maintain 1:1 aldehyde:hydroxylamine ratios. Precursor solutions were dissolved in saline (60 °C for 3 h; then at 25 °C overnight), mixed at 80:20 (MN systems) or 50:50 (FITC-SPIF systems) volume ratios via luer-lock syringes, and moulded. Crosslinking leveraged oxime bond formation, enhancing hydrolytic stability.

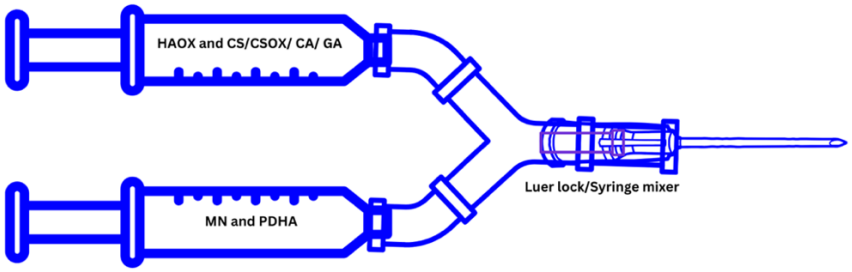

Fig. 3.1: Schematic of a pair-syringe system connected by a luer lock adapter or mixing port used in the crosslinking process of HAOX and HAOX-CSOX hydrogel.

$$C_w^{PDHA} = \frac{C_w^{HAOX} . V_{HAOX} . M_{PDHA} . DS_{HAOX}}{V_{PDHA} . P . P_p . M_{HAOX}} \quad (3.2)$$

In this context, C_w^{HAOX} represents the HAOX mass concentration (w/v) in the first syringe, DS_{HAOX} denotes the degree of substitution of HAOX, P refers to the ratio of aldehyde to hydroxylamine groups, which is set to 1. P_p indicates the number of hydroxylamine groups in PDHA (2), V_{HAOX} is the volume of HAOX solution in the first syringe, V_{PDHA} is the total volume of MN mixed with PDHA solution, M_{PDHA} is the molar mass of PDHA (179 g mol^{-1}), and M_{HAOX} is the molar mass of the HA disaccharide unit (400 g mol^{-1}).

$$C_w^{PDHA} = \left(\frac{C_w^{HAOX} . V_{HAOX} . M_{PDHA} . DS_{HAOX}}{V_{PDHA} . P . P_p . M_{HAOX}}\right) + \left(\frac{C_w^{CSOX} . V_{CSOX} . M_{PDHA} . DS_{CSOX}}{V_{PDHA} . P . P_p . M_{CSOX}}\right) \quad (3.3)$$

The values in the second set of parentheses correspond to the CSOX analogues of those in the first set, where M_{CSOX} represents the molar mass of CSOX disaccharide unit (600 g mol^{-1}).

Table 3.1 Series of studied formulations for MN-DDS.

Formulations	HAOX (mg mL^{-1})	CSOX (mg mL^{-1})	CS (mg mL^{-1})	CA (□M)	GA (mg mL^{-1})	PDHA (mg mL^{-1})	MN (□g mL^{-1})
HAOX	20	-	-	-	-	0.32	-
CSOX-MN	-	100	-	-	-	1.865	200
HAOX-MN	20	-	-	-	-	0.32	200
HAOX-CHELATE	20	-	-	7.2	-	0.32	200
HAOX_PECS (unbound PEC)	20	-	5	7.2	1	0.32	200
HAOX_PECOX (immobilized PEC)	20	5	-	7.2	1	0.462	200

Table 3.2 Formulations for designing a suitable delivery system for SPIF.

Formulations	HAOX (mg mL^{-1})	CSOX (mg mL^{-1})	FITC-SPIF (□g mL^{-1})	PDHA (mg mL^{-1})	pH
HAOX_15	20	0	100	0.32	5
HACOX_25	15	5	100	0.39	5
HACOX_35	10	10	100	0.465	5
HAOX_17	20	0	100	0.32	6.8
HACOX_27	15	5	100	0.39	6.8
HACOX_37	10	10	100	0.465	6.8

Table 3.3 Development of HACOX_37: Influence of FITC-SPIF loading levels on CDR, swelling behaviour, and Korsmeyer-Peppas modelling.

Formulations	HAOX (mg mL^{-1})	CSOX (mg mL^{-1})	FITC-SPIF (□g mL^{-1})	PDHA (mg mL^{-1})	pH
HACOX_37	10	10	100	0.465	6.8
HACOX_37_250	10	10	250	0.465	6.8
HACOX_37_500	10	10	500	0.465	6.8

Table 3.4 Development of HACOX_37: Influence of CSOX concentration on CDR, swelling behaviour, and Korsmeyer-Peppas modelling.

Formulations	HAOX (mg mL^{-1})	CSOX (mg mL^{-1})	FITC-SPIF (□g mL^{-1})	PDHA (mg mL^{-1})	pH
HACOX_37_250	10	10	250	0.465	6.8
HACOX_47_250	10	20	250	1.49	6.8
HACOX_57_250	10	30	250	2.11	6.8

3.2 Characterization techniques

3.2.1 Gelation time

The gelation time measured via rheometry (Discovery Hybrid Rheometer–3, TA Instruments) using oscillatory time sweeps (25 °C, 5% strain, 1 Hz). Gelation onset was defined by the cross over point of the G’ and G”.

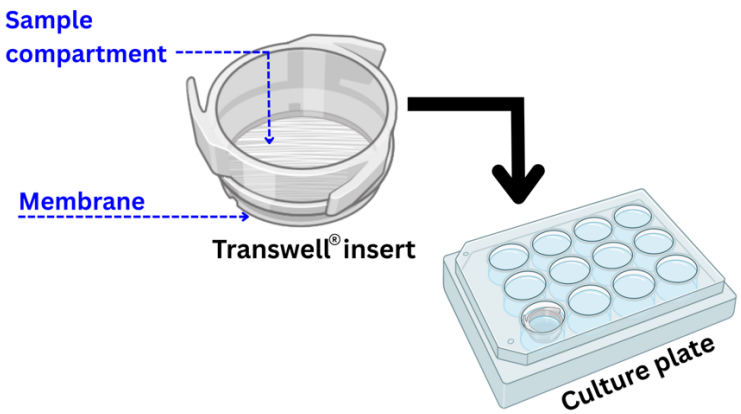

Fig. 3.2: Illustration of Transwell® system. A porous membrane separates two chambers, with DMTs-loaded DDS introduced in the upper compartment and drug release is quantified in the lower compartment.

3.2.2 Swelling ratio (Q)

Calculated gravimetrically (Equation 3.4) using Transwell® inserts (Fig. 3.2). Hydrogels were immersed in saline (MN systems) or PBS (FITC-SPIF systems) at 37 °C, with mass recorded at 1, 3, 7, 10, and 14 days.

$$Q = \frac{(m_t - m_r)}{m_r} \times 100\% \quad (3.4)$$

3.2.3 Drug release experiment

The release was evaluated *in vitro* using a Transwell® set up (Fig. 3.2). MN was quantified using HPLC (Waters, UPLC system equipped with a PDA-QDA detector), while FITC-SPIF was measured using UV-vis. Cumulative release (CDR, equation 3.5) was modelled using the Korsmeyer-Peppas equation (Equation 3.6) to classify diffusion mechanisms.

$$CDR = \frac{m_t}{m_\infty} \times 100\% \quad (3.5)$$

$$kt^n = \frac{m_t}{m_\infty} \quad (3.6)$$

The equation allowed for the estimation of both the diffusion factor (n) and the kinetics constant (k), which are influenced by the design and spatial configuration of the delivery matrix. An $n \leq 0.5$ signifies Fickian diffusion, while $0.5 \leq n \leq 1$ is indicative of anomalous (non-Fickian) transport, the $n = 1$ corresponds to case-II transport, and $n \geq 1$ is associated with super case-II.

3.2.4 Injectability

The ease of injection was assessed using Instron 3342 Single Column Materials Testing System (18-20 G needles, equipped with a 100 N compression plate at a speed of 50 mm/min. Parameters such as injection pressure, plunger displacement, dynamic glide force (*DGF*), and maximum force ($F_{\max}$) were quantified using Bluehill software.

3.2.5 Bioactivity assays

- MN – bioactivity was assessed using the Whole Blood Monocytes Activation Test (WB-MAT), using a modified protocol adapted from previously established methods [45,46]. Heparinized whole blood from healthy donors was stimulated with LPS (0.25 - 5 IU mL^{-1}) and treated with MN released from the DDS. IL-6 suppression was quantified via ELISA (Invitrogen kit) after 24 h incubation at 37 °C.
- FITC-SPIF bioactivity was assessed by measuring the immunomodulation of THP-1 macrophages, using a macrophage-based inflammation model, with adjustment made as outlined in reference [47]. Macrophage differentiation was initiated by 72-h exposure to 100 nM PMA. After differentiation, the cells were pretreated for 48 h with either fresh solution of FITC-SPIF or FITC-SPIF released from the DDS, then stimulated with TNF-α (100 ng mL^{-1}). qRT-PCR was used to analysed pro-inflammatory genes and anti-inflammatory genes at 0 h (baseline) and 6 h post- TNF-α.

3.3 Data processing and statistical approaches

Data were analysed by one-way analysis of variance (ANOVA), considering p-value < 0.05 as statistically significant. Asterisks denote significance levels as follow: * for $p \leq 0.05$, ** for $p \leq 0.01$, *** for $p \leq 0.001$, **** $p \leq 0.00001$, ns for non-significant. Sample size is represented as “n”.

For comprehensive protocols (e.g., SEC-MALLS parameters, qPCR probe sequences, detailed formulations, preparation steps, characterizations, refer to the original document.

4. RESULT AND DISCUSSION

4.1 In situ injectable hyaluronic acid hydrogel loaded with polyelectrolyte complex for minocycline control release

The clinical application of MN in MS is restricted by its pharmacokinetic drawbacks and burdensome administration, making advanced delivery technologies essential to improve therapeutic outcomes. To mitigate these concerns, this study introduces an injectable hydrogel system incorporating PEC to localize and modulate MN's release. HAOX serves as a base component for the whole DDS to be injectable and stationary, and CS or CSOX provides a high binding affinity for Ca^{2+}. Particularly for CSOX, it also serves as a crosslinkable structure to form immobilized PEC. This DDS leverages a combination of crosslinkable biopolymers to reduce the burst release commonly associated with conventional formulations, thereby prolonging the therapeutic window and improving compliance.

4.1.1 Synthesis of aldehyde-modified chondroitin sulfate (CSOX)

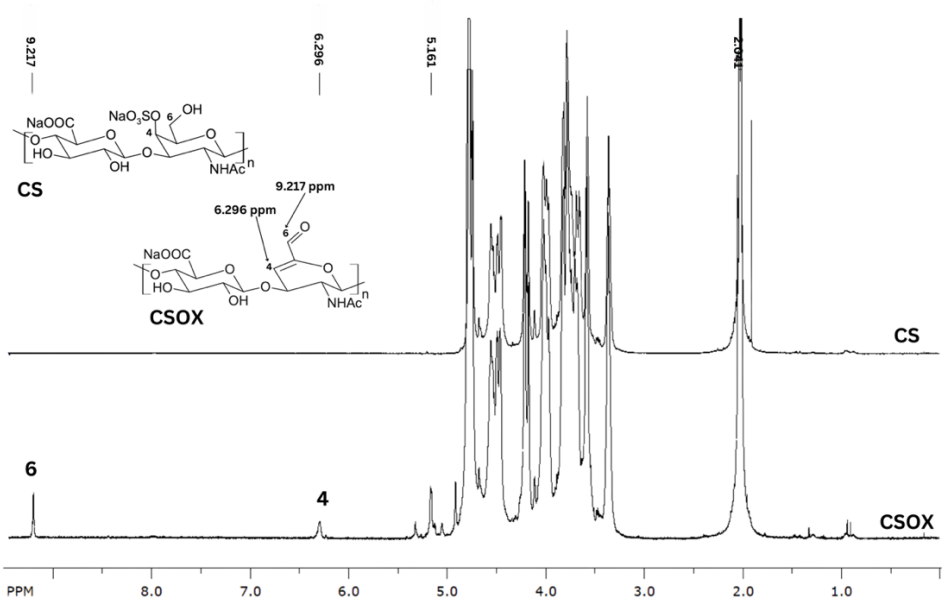

Fig. 4.1: ^{1}H NMR of aldehyde modified chondroitin sulfate.

^{1}H NMR confirmed the characterization of the CSOX structure by focusing on the proton signals corresponding to the C-4 and C-6 positions, as well as the saturated carboxyl group, which exhibited chemical shifts at 6.296 ppm and 9.217 ppm, respectively (see Fig. 4.1). The spectra showed that the oxidation process with 0.5 molar equivalents of NaClO produced CSOX with a DF of approximately 20%. Furthermore, SEC-MALLS determined the CSOX's molecular mass to be around 12 kDa.

4.1.2 Gelation duration and injectability of HAOX-based DDS

Gelation time, pivotal for ensuring injectability and structural integrity, varied significantly across formulations. HAOX and its engineered variants (HAOX-MN, HAOX_PECS, and HAOX_PECOX) achieved rapid gelation within 33 – 50 s (Fig. 4.2). This rapid gelation is consistent with previous studies on HAOX-based systems [48,49], where the high concentration of reactive aldehyde groups in HAOX facilitates efficient crosslinking with PDHA, leading to quick network formation. The 30-50 s gelation window observed for HAOX, HAOX-MN, HAOX_PECS, and HAOX_PECOX corresponds to established clinical benchmarks [50], supporting their suitability for injectable DDS.

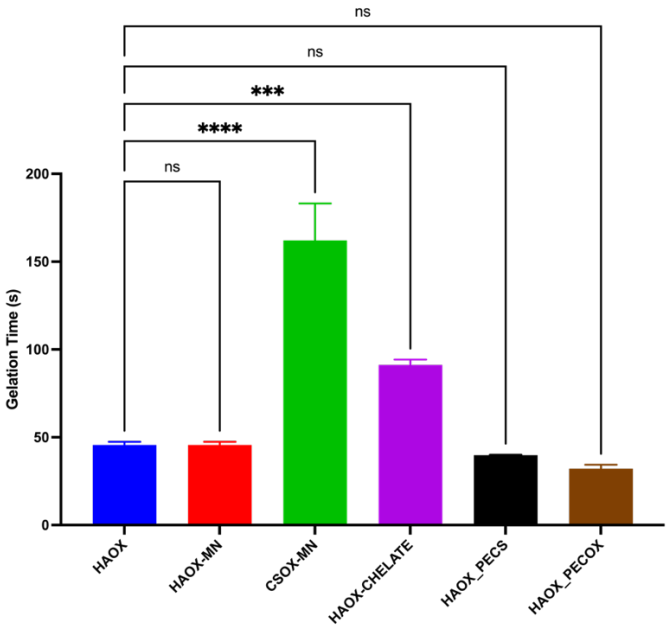

*Fig. 4.2: Comparative assessment of gelation profile for hydrogels based on CSOX, HAOX, and PEC (unbound and immobilized). Result from triplicate trials (n =3) show **** $p < 0.0001$ for CSOX-MN versus PURE HAOX).*

Table 4.1 Injectability assessment of HAOX_PECOX formulation using dynamic glide force (DGF) and maximum force (F_{max}) metrics (n=3).

Formulation	**Needle size (G)**	**⌀ (mm)**	P_{max} **[kPa]**	F_{max} **[N]**
HAOX_PECOX	18	1.27	358 ± 33	5.8 ± 0.3
	19	1.07	494 ± 67	7.8 ± 1.1
	20	0.9	577 ± 13	9.0 ± 0.2

Symbol definition:
⌀ = Inner diameter of the needle.

Injectability analysis of HAOX_PECOX demonstrated a robust linear correlation between decreasing needle diameter and increasing DGF, adhering to

Hagen-Poiseuille principles (Table 4.1). For 20 G needle, measured values of F_{max}= (9.0 ± 0.2) N and DGF = (8.0 ± 1.0) N remained below the established 40 N patient comfort threshold [50].

4.1.3 Minocycline release profiles and the mechanism in injectable HAOX-based drug delivery system

The HAOX-MN formulation exhibited rapid burst release (50% MN within 24 h; Fig. 4.3 b), attributable to HAOX hydrophilicity and weak drug-polymer interactions. In contrast, CSOX-MN formulation minimized burst release (2.5% in 24 h; Fig. 4.3 b) through electrostatic interactions between MN's amine groups and CSOX's sulfate moieties. The HAOX_PECOX formulation addressed these limitations by immobilizing PECs withing HAOX matrix by substituting CS with CSOX. This approach reduced burst release to 23.6% ($p < 0.001$ vs HAOX-MN; Fig. 4.3 b), achieving 65% cumulative release over 288 h (Fig. 4.3 a).

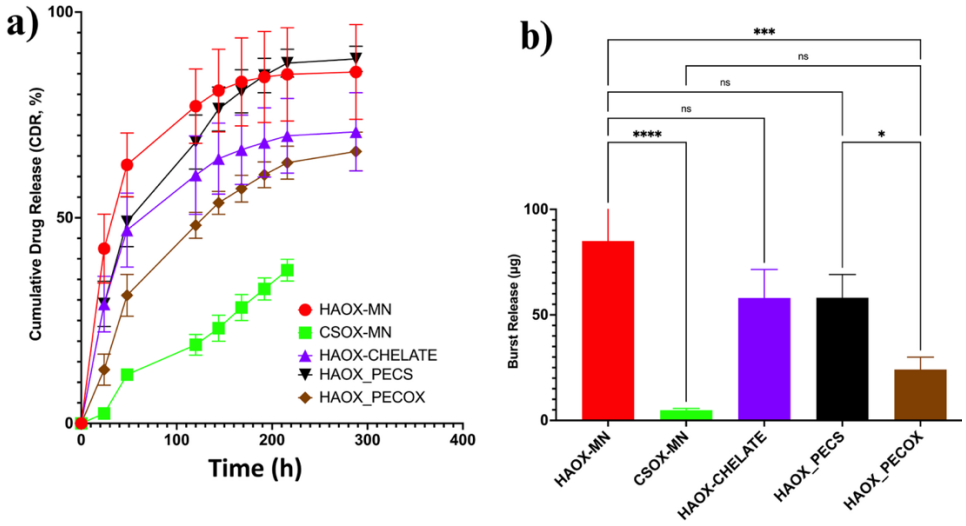

*Fig. 4.3: Sustained and burst-release patterns of minocycline from DDS: Subfigure (a) illustrates time-dependent CDR for HAOX-CSOX hydrogels; Subfigure (b) quantifies burst-release. Statistical analysis (n=3): ** $p < 0.01$, *** $p < 0.001$, ns is non-significant.*

Table 4.2 Korsmeyer-Peppas release fitting across formulations.

Formulations	k	n	R^2
HAOX-MN	0.188 ± 0.07	0.299 ± 0.08	0.994
CSOX-MN	n.a	n.a	n.a
HAOX-CHELATE	0.135 ± 0.04	0.311 ± 0.04	0.991
HAOX_PECS	0.087 ± 0.01	0.461 ± 0.01	0.992
HAOX_PECOX	0.054 ± 0.02	0.520 ± 0.07	0.991

Mechanistic analysis employed the Korsmeyer-Peppas model to quantify release dynamic through the rate constant (k) and diffusion exponent (n) [43,48,49]. HAOX-MN (k = 0.188) and HAOX-CHELATE (k = 0.135; Table 4.2) revealed Fickian diffusion (n < 0.5; Table 4.2), indicating MN transport dominated by concentration gradient rather than other mechanisms, such as matrix erosion. Analogous Fickian release kinetics associated with weak drug-polymer interactions have been documented in similar systems [36,51]. Meanwhile, HAOX_PECS demonstrated anomalous transport (n = 0.520) through combined diffusion and several other intrinsic process, including polymer relaxation and PEC decomplexation [38,52] (Table 4.2).

4.1.4 The influence of swelling behaviour on sustained MN release in hydrogel-based delivery system

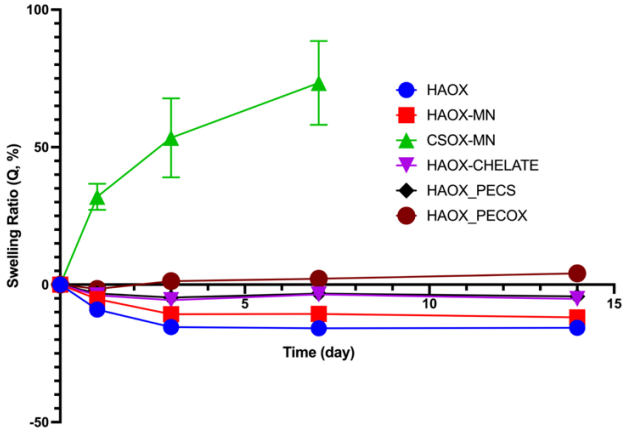

Fig. 4.4:Quantitative swelling profile of DDS formulations (swelling ratio vs. time; n=3).

Swelling analysis revealed distinct hydration mechanisms across formulations (Fig. 4.4). HAOX-based hydrogels universally displayed low to non-swelling characteristics, analogous to phenomena reported in crosslinked HA systems [39,48,49,53]. HAOX_PECOX exhibited a slightly higher rate of water uptake despite higher crosslinking density (Fig. 4.5). The immobilized PECs in HAOX_PECOX create electrostatic barriers between sulfate anions and protonated MN at physiological pH, effectively decelerating MN diffusion. Conversely, HAOX-MN's lack of ionic modifiers results in unhindered MN mobility. These findings underscore the proposed contribution of this work: the development of HAOX_PECOX, a formulation that leverages immobilized PECs to reconcile conflicting demands of structural stability and sustained release.

4.2 In situ forming hydrogel from aldehyde-modified hyaluronic acid and aldehyde-modified chondroitin sulfate for synthetic preimplantation factor delivery

Recent advancements highlight SPIF's therapeutic promise in addressing neuroinflammatory disease, particularly MS. Despite its potential to cross the BBB and modulate inflammation, its clinical application is hindered by challenges such as enzymatic degradation, short biological half-life, and the need for frequent systemic dosing, which can lead to poor patient adherence and suboptimal therapeutic outcomes. Building on the application of immobilized PEC within HAOX hydrogel for controlled MN release, this study investigates the adaptability of the system for FITC-SPIF delivery. HAOX serves as the primary component, ensuring injectability and mechanical stability, while the amine residues of FITC-SPIF (presented by lysine and arginine) interact electrostatically with the sulfate groups of CSOX to form PEC.

4.2.1 Gelation time of FITC-SPIF-loaded HAOX-CSOX hydrogels: balancing pH-dependent crosslinking for clinical translation

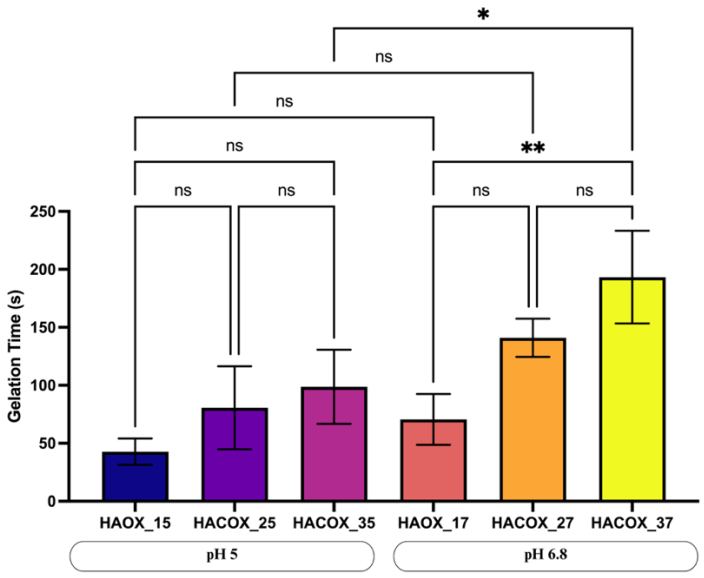

Fig. 4.5: Gelation time of injectable hydrogels containing FITC-SPIF, measured at two preparation pH values (5.0 and 6.8). Each group includes three formulations with increasing CSOX concentrations: no CSOX (HAOX_15 at pH 5, HAOX_17 at pH 6.8), 0.5% CSOX (HACOX_25, HACOX_27), and 1% CSOX (HACOX_35, HACOX_37). Results represent mean ± SD (n = 3).

The gelation behaviour of HAOX-CSOX hydrogels was profoundly influenced by preparation pH and CSOX concentration, with distinct mechanisms governing network formation under acidic (pH 5) and near-physiological (pH 6.8) conditions (Fig. 4.5). At pH 5, hydrogels exhibited rapid and uniform gelation (74 ± 3 s, $p >$ 0.05 across CSOX concentrations), driven by acid-catalysed oxime bond formation between HAOX aldehydes and the crosslinker PDHA. In contrast, at

pH 6.8, gelation times varied significantly, ranging from 70 s for HAOX-only formulations (HACOX_17) to 193 s for CSOX-rich systems (HACOX_37, $p < 0.01$). The 193 s gelation time observed for HACOX_37 at pH 6.8 aligns with literature-reported ideals (3–5 minutes) for injectable systems concerning the balance between syringe-ability and injectability [54].

4.2.2 Release study of FITC-SPIF, T50 %, and Korsmeyer-Peppas parameters

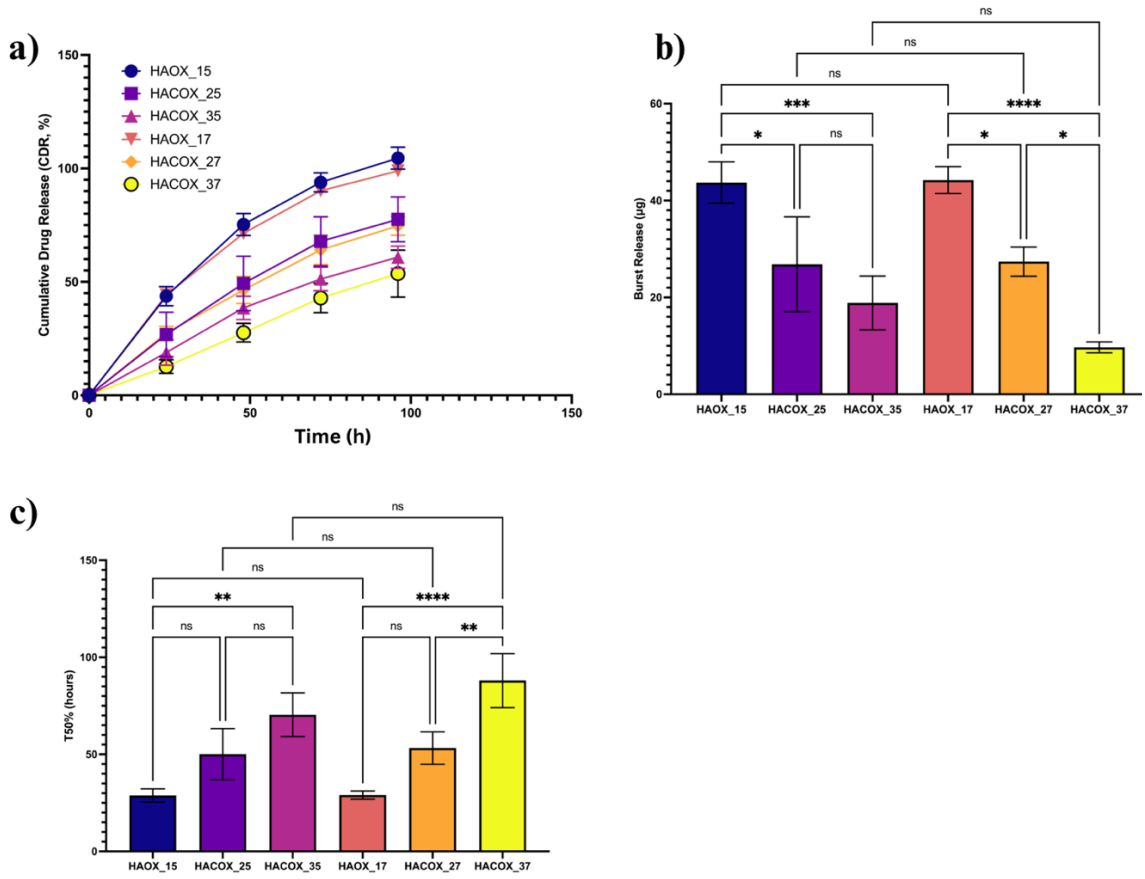

Fig. 4.6: *Drug release profile across different preparation pH and formulation, a) cumulative drug release, b) burst profile, c) T50%. Data are expressed as mean ± SD (n = 3). Significance levels: *p < 0.05, **p < 0.01, ***p < 0.001, ****p < 0.0001, ns = non-significant.*

UV-Vis analysis revealed that CSOX concentration serves as a critical determinant of burst release characteristics (Fig. 4.6). Control formulations lacking CSOX (HAOX_15 and HAOX_17) exhibited high burst, releasing 43–44 µg of FITC-SPIF during the initial 24 h, followed by sustained daily release of 18–20 µg. Further increasing CSOX to 1% enhanced burst suppression markedly: HACOX_35 and HACOX_37 demonstrated 58% and 78% reductions ($p < 0.001$), respectively, followed by controlled daily release of 14 µg and 13 µg. These findings provide evidence for the role of CSOX in enhancing electrostatic interactions that promote FITC-SPIF retention within the hydrogel network.

Mechanistic analysis using the Korsmeyer-Peppas model (Table 4.3) yielded diffusional exponent values (n) between 0.692 - 0.917. These values indicate anomalous transport behaviour, where drug release is not exclusively dependent on diffusion but is also modulated by additional variables such as solubility, crosslinking density, matrix composition, and intermolecular interactions between FITC-SPIF and the polymeric matrix within the DDS. The kinetic constant (k) exhibited an inverse relationship with CSOX concentration, decreasing by up to 84% in high-CSOX formulations (Table 4.4).

Table 4.3 Korsmeyer-Peppas kinetic modelling of FITC-SPIF release from DDS prepared at varied pH levels (n=3).

Formulations	k	n	R^2
HAOX_15	0.037 ± 0.01	0.783 ± 0.05	0.999
HACOX_25	0.020 ± 0.02	0.833 ± 0.16	0.999
HACOX_35	0.018 ± 0.01	0.761 ± 0.08	0.997
HAOX_17	0.050 ± 0.01	0.692 ± 0.07	1.000
HACOX_27	0.025 ± 0.01	0.764 ± 0.09	0.999
HACOX_37	0.008 ± 0.01	0.917 ± 0.08	0.997

4.2.3 Swelling profile and crosslinking density of the drug delivery system

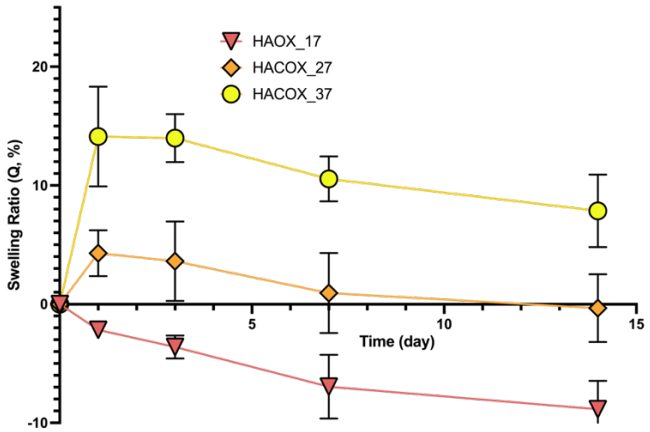

Fig. 4.7: Swelling ratio of formulation prepared at pH 6.8 (n=3).

Increasing CSOX concentration reduces crosslinking density while enhancing swelling capacity (Fig. 4.7). The minimal to non-swelling characteristics observed across formulations contrast significantly with traditional HA-based hydrogels [55–57]. For instance, HACOX_37's lower crosslinking density allows greater swelling, yet its sulfate-mediated electrostatic interactions with FITC-SPIF mitigate rapid drug release. This dual functionality obtained by combining covalent stability with tuneable hydration, resolves the historical compromise between hydrogel swelling and drug retention.

4.2.4 Injectability of the drug delivery system

The injectability of the HAOX-CSOX hydrogel system represent a critical advancement in addressing the dual demands of mechanical stability and patient-centric administration for MS therapy. HACOX_37 achieves injectability within clinically acceptable thresholds (sustained dispensing force = 2.8 N; peak injection force = 2.9 N; Table 4.4), directly addressing MS patients' preference for minimally invasive therapies [58,59].

Table 4.4 Injectability parameters of HACOX_37, evaluated through dynamic glide force (DGF) and maximum extrusion force (Fmax) (n=3).

Formulation	**Needle size (G)**	**Duration from crosslinking process (s)**	P_{max} **[kPa]**	**DGF (N)**	F_{max} **[N]**
HACOX_37	27	60	185 ± 22	2.8 ± 0.5	3.1 ± 0.3
		180	192 ± 25	2.89 ± 0.4	2.9 ± 0.4

4.2.5 FITC-SPIF-induced macrophage polarization: an in vitro bioactivity study

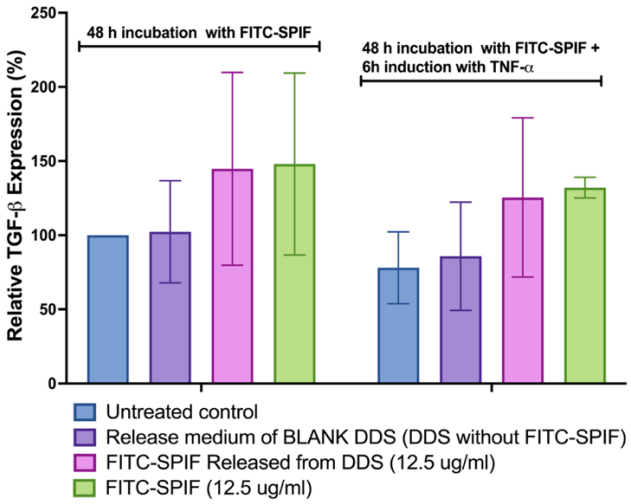

Fig. 4.8: TGF-β expression after treatment with FITC-SPIF.

FITC-SPIF uniquely induced a significant increase in TGF-β expression ($p < 0.05$) (Fig. 4.8), regardless of delivery method (free peptide vs. HACOX_37-released). This selective TGF-β upregulation (absent in blank hydrogel controls) suggests a selective macrophage polarization shift toward an M2 phenotype, potentially enabling tissue repair and immunoregulation. The HAOX-CSOX hydrogel successfully preserved FITC-SPIF bioactivity, a critical outcome of its design where PDHA-mediated covalent crosslinking stabilizes against enzymatic degradation while localized delivery prevents systemic dilution. This strategy

overcomes limitations of conventional DMTs [60]. However, our *in vitro* model revealed constraints: the absence of VCAM-1 inhibition and isolated suppression of PTGS2 (prostaglandin synthase) underscore the limitations of *in vitro* models in replicating SPIF's multifaceted in vivo effects (embryo protection and neuro-restoration) [29,30].

5. CONCLUSIONS

Managing MS remains challenging, as current DMTs rely heavily on patient adherence despite their clinical benefits. Frequent dosing and cognitive demands can burden patients, especially those with fatigue or impairments. Additionally, conventional DMTs often face limitations such as poor pharmacokinetics, fluctuating plasma levels, and increased systemic side effects. An implantable DDS could address these issues by enabling sustained, localized release with minimal patient involvement, providing features strongly preferred by people with MS. This work focuses on addressing the patient's preferences through the design of an injectable hydrogel platform combining HAOX and CSOX. The injectability characteristics of this system allow it to be administered either to implantable devices or directly to the host tissue. The HAOX-CSOX system leverages covalent crosslinking with PDHA to immobilize PECs, creating a structurally stable network capable of entrapping both small molecules (e.g., MN) and short peptides (e.g., FITC-SPIF). By integrating electrostatic interactions, covalent bonding, and tuneable mechanical properties, the platform achieves precise control over drug release kinetics while preserving structural integrity and bioactivity.

The synthesis of CSOX was optimized through a one-pot reaction strategy under mild alkaline conditions. This approach enabled simultaneous oxidation and functionalization of CS, yielding a derivative with a molecular mass of 12 kDa and a 20% degree of functionalization. The preservation of CS's pyranose ring during synthesis ensured biocompatibility and mechanical robustness, while the introduction of aldehyde groups facilitate the immobilization of CSOX onto HAOX matrices via PDHA.

For MN delivery, PECs were formed through electrostatic interactions between MN's positively charged amine groups, GA, CA, and the sulfate groups of CSOX. Subsequent covalent crosslinking with PDHA to HAOX stabilized the structure, reducing burst release by 88% compared to unbound PECs and extending the half-release period (T50%) to 127 h. This prolonged release profile is attributed to the synergistic mechanism: the immobilized PEC acts as a primary reservoir responsible for tuning the release kinetic, while the HAOX matrix provides injectable and localised compartment. Clinically viable for patient-friendly administration, the system's viscoelastic properties and low extrusion forces facilitate smooth injection through a 20-gauge needle. The released MN

demonstrated a significant 56% suppression of LPS-stimulated IL-6 production, validating HAOX-PEC hydrogel as effective delivery platforms.

For peptide delivery, the system was adapted to accommodate FITC-SPIF. By modulating CSOX concentration, drug entrapment efficiency was maximized, and burst release was reduced from 38% to 78%. Crucially, released FITC-SPIF retained its bioactivity, as evidenced by its ability to induce TGF-β secretion in macrophages. Furthermore, the HAOX-CSOX hydrogel distinguishes itself through its simplicity and versatility. Unlike nanoparticle-based systems, this platform relies on straightforward polymer interactions to form PEC. The absence of organic solvents preserves drug integrity.

The insights gained from this study reveal the platform's potential to meet essential drug delivery objectives for chronic inflammatory conditions like MS. The system achieves prolonged, controlled drug release, ensuring sustained therapeutic levels while significantly reducing the need for frequent patient involvement. By leveraging a synergistic mechanism of immobilized and maintaining structural integrity, the platform minimizes dosing frequency. The system enables localized delivery, confining drug activity to the target site and thereby reducing systemic toxicity. The platform's compatibility with diverse therapeutics has been demonstrated through its adaptability to both small molecules and peptides. Finally, the system prioritizes minimally invasive administration, offering patient-friendly features such as smooth injectability and rapid gelation.

This study demonstrates the translational potential of hydrogels for sustained drug delivery in MS, yet clinical applicability hinges on overcoming critical preclinical challenges. Future work must prioritize targeted efficacy metrics and safety profiling to address risks of degradation byproduct accumulation. Strategically integrating these systems with existing DMTs could further refine therapeutic precision. Ultimately, bridging the gap between engineered solutions and clinical viability will require interdisciplinary collaboration. This research advances the field by introducing a paradigm-shifting approach through the innovative HAOX-CSOX hydrogel platform. It addresses the critical limitations of current systems, including patient adherence challenges and systemic toxicity. The platform's ability to deliver sustained, localized therapy while accommodating diverse drug classes underscores its potential to redefine standards in personalized medicine.

REFERENCES

[1] A. Alhazzani, M. Alqahtani, N. Alamri, L. Sarhan, S. Alkhashrami, M. Alahmarii, Treatment satisfaction and adherence to medications among multiple sclerosis patients in Saudi Arabia, Egyptian Journal of Neurology, Psychiatry and Neurosurgery 55 (2019) 1–7. https://doi.org/10.1186/s41983-019-0095-6.

[2] M.K. Sen, M.S.M. Almuslehi, P.J. Shortland, J.R. Coorssen, D.A. Mahns, Revisiting the Pathoetiology of Multiple Sclerosis: Has the Tail Been Wagging the Mouse?, Front Immunol 11 (2020) 1–9. https://doi.org/10.3389/fimmu.2020.572186.

[3] D. Bandari, M. Adamson, M. Bowman, A. Gutierrez, A. Athavale, B. Oak, N. Hadker, F. Branco, C. Geremakis, J.B. Lewin, S.L. Shankar, Real-world treatment preferences among health care providers in the United States in selecting disease modifying therapies for patients with multiple sclerosis: a discrete choice experiment, J Med Econ 26 (2023) 1507–1518. https://doi.org/10.1080/13696998.2023.2279883.

[4] A. Kołtuniuk, J. Chojdak-łukasiewicz, Adherence to Therapy in Patients with Multiple Sclerosis—Review, Int J Environ Res Public Health 19 (2022) 1–9. https://doi.org/10.3390/ijerph19042203.

[5] J.A. Nicholas, N.C. Edwards, R.A. Edwards, A. Dellarole, M. Grosso, A.L. Phillips, Real-world adherence to, and persistence with, once- and twice-daily oral disease-modifying drugs in patients with multiple sclerosis: A systematic review and meta-analysis, BMC Neurol 20 (2020) 1–15. https://doi.org/10.1186/s12883-020-01830-0.

[6] N. Poudel, B. Banjara, S. Kamau, N. Frost, S. Ngorsuraches, Factors influencing patients' willingness-to-pay for disease-modifying therapies for multiple sclerosis, Mult Scler Relat Disord 48 (2021) 1–5. https://doi.org/10.1016/j.msard.2020.102720.

[7] B. Bauer, B. Brockmeier, V. Devonshire, A. Charbonne, D. Wach, B. Hendin, An international discrete choice experiment assessing patients' preferences for disease-modifying therapy attributes in multiple sclerosis, Neurodegener Dis Manag 10 (2020) 369–382. https://doi.org/10.2217/nmt-2020-0034.

[8] EMSP, MS Barometer 2020: Assessing the gaps in care for people with multiple sclerosis across Europe, Brussels, 2021. http://msbarometer.com/.

[9] M. Biolato, A. Bianco, M. Lucchini, A. Gasbarrini, M. Mirabella, A. Grieco, The Disease-Modifying Therapies of Relapsing-Remitting Multiple Sclerosis and Liver Injury: A Narrative Review, CNS Drugs 35 (2021) 861–880. https://doi.org/10.1007/s40263-021-00842-9.

[10] M. Moccia, I. Loperto, R. Lanzillo, A. Capacchione, A. Carotenuto, M. Triassi, V. Brescia Morra, R. Palladino, Persistence, adherence, healthcare resource utilisation and costs for interferon Beta in multiple sclerosis: A population-based study in the Campania region (southern Italy), BMC Health Serv Res 20 (2020) 1. https://doi.org/10.1186/s12913-020-05664-x.

[11] C. Dello Russo, K.A. Scott, M. Pirmohamed, Dimethyl fumarate induced lymphopenia in multiple sclerosis: A review of the literature, Pharmacol Ther 219 (2021) 1–18. https://doi.org/10.1016/j.pharmthera.2020.107710.

[12] T.L. Vollmer, J.A. Cohen, E. Alvarez, K. V. Nair, A. Boster, J. Katz, G. Pardo, J. Pei, P. Raut, S. Merchant, E. MacLean, A. Pradhan, B. Moss, Safety results of administering ocrelizumab per a shorter infusion protocol in patients with primary progressive and relapsing multiple sclerosis, Mult Scler Relat Disord 46 (2020) 1–6. https://doi.org/10.1016/j.msard.2020.102454.

[13] C. Kang, H.A. Blair, Ofatumumab: A Review in Relapsing Forms of Multiple Sclerosis, Drugs 82 (2022) 55–62. https://doi.org/10.1007/s40265-021-01650-7.

[14] M. Paz-Zulueta, P. Parás-Bravo, D. Cantarero-Prieto, C. Blázquez-Fernández, A. Oterino-Durán, A literature review of cost-of-illness studies on the economic burden of multiple sclerosis., Mult Scler Relat Disord 43 (2020) 1–9. https://doi.org/10.1016/j.msard.2020.102162.

[15] N.A. Gallehzan, M. Khosravi, K. Jamebozorgi, N. Mir, H. Jalilian, S. Soleimanpour, S. Hoseini, A. Rezapour, A. Eshraghi, Cost-utility and cost-effectiveness analysis of disease-modifying drugs of

relapsing–remitting multiple sclerosis: a systematic review, Health Econ Rev 14 (2024) 1–37. https://doi.org/10.1186/s13561-024-00478-7.

[16] G. Vorobeychik, D. Black, P. Cooper, A. Cox, Multiple Sclerosis and Related Challenges to Young women's Health: Canadian Expert Review, Neurodegener Dis Manag 10 (2020) 1–13. https://doi.org/10.2217/nmt-2020-0010.

[17] M.C. De Rosa, R. Purohit, A.T. García-Sosa, Drug repurposing: a nexus of innovation, science, and potential, Sci Rep 13 (2023) 1–3. https://doi.org/10.1038/s41598-023-44264-7.

[18] S. Cheng, J. Hou, C. Zhang, C. Xu, L. Wang, X. Zou, H. Yu, Y. Shi, Z. Yin, G. Chen, Minocycline reduces neuroinflammation but does not ameliorate neuron loss in a mouse model of neurodegeneration, Sci Rep 5 (2015) 1–11. https://doi.org/10.1038/srep10535.

[19] E.J. Clarke, L.A. Vodstrcil, E.L. Plummer, I. Aguirre, R.S. Samra, C.K. Fairley, E.P.F. Chow, C.S. Bradshaw, Efficacy of Minocycline for the Treatment of Mycoplasma genitalium, Open Forum Infect Dis 10 (2023) 1–7. https://doi.org/10.1093/ofid/ofad427.

[20] B. Wang, W. Lin, H. Zhu, Minocycline improves the recovery of nerve function and alleviates blood-brain barrier damage by inhibiting endoplasmic reticulum in traumatic brain injury mice model, Eur J Inflamm 19 (2021) 1–12. https://doi.org/10.1177/20587392211010898.

[21] P.J. Bergold, R. Furhang, S. Lawless, Treating Traumatic Brain Injury with Minocycline, Neurotherapeutics 20 (2023) 1546–1564. https://doi.org/10.1007/s13311-023-01426-9.

[22] C. Wei, Y. Liu, A. Jiang, B. Wu, A pharmacovigilance study of the association between tetracyclines and hepatotoxicity based on Food and Drug Administration adverse event reporting system data, Int J Clin Pharm 44 (2022) 709–716. https://doi.org/10.1007/s11096-022-01397-5.

[23] J. Zhang, M. Boska, Y. Zheng, J. Liu, H.S. Fox, H. Xiong, Minocycline attenuation of rat corpus callosum abnormality mediated by low-dose lipopolysaccharide-induced microglia activation, J Neuroinflammation 18 (2021) 1–11. https://doi.org/10.1186/s12974-021-02142-x.

[24] H.F. Elewa, R. Hilali, D.C. Hess, L.S. Machado, S.C. Fagan, Minocycline for short-term neuroprotection, Pharmacotherapy 26 (2006) 515–521. https://doi.org/10.1592/phco.26.4.515.

[25] L.M. Metz, D.K.B. Li, A.L. Traboulsee, P. Duquette, M. Eliasziw, G. Cerchiaro, J. Greenfield, A. Riddehough, M. Yeung, M. Kremenchutzky, G. Vorobeychik, M.S. Freedman, V. Bhan, G. Blevins, J.J. Marriott, F. Grand'Maison, L. Lee, M. Thibault, M.D. Hill, V.W. Yong, Trial of Minocycline in a Clinically Isolated Syndrome of Multiple Sclerosis, New England Journal of Medicine 376 (2017) 2122–2133. https://doi.org/10.1056/nejmoa1608889.

[26] A.D. Holmkvist, A. Friberg, U.J. Nilsson, J. Schouenborg, Hydrophobic ion pairing of a minocycline/Ca2+/AOT complex for preparation of drug-loaded PLGA nanoparticles with improved sustained release, Int J Pharm 499 (2016) 351–357. https://doi.org/10.1016/j.ijpharm.2016.01.011.

[27] D. Manoharan, S. Srinivasan, N.R. Vignesh, A. Senthilvel, Tetracyclines: The Old, the New and the Improved - A Short Review, Biomedical and Pharmacology Journal 16 (2023) 1441–1450. https://doi.org/10.13005/bpj/2722.

[28] S. Hayrabedyan, R. Shainer, Z. Yekhtin, L. Weiss, O. Almogi-Hazan, R. Or, C.L. Farnsworth, S. Newsome, K. Todorova, M.J. Paidas, C. Brodie, E.R. Barnea, M. Mueller, Synthetic PreImplantation Factor (sPIF) induces posttranslational protein modification and reverses paralysis in EAE mice, Sci Rep 9 (2019) 1–10. https://doi.org/10.1038/s41598-019-48473-x.

[29] M. Spinelli, C. Boucard, F. Di Nicuolo, V. Haesler, R. Castellani, A. Pontecorvi, G. Scambia, C. Granieri, E.R. Barnea, D. Surbek, M. Mueller, N. Di Simone, Synthetic PreImplantation Factor (sPIF) reduces inflammation and prevents preterm birth, PLoS One 15 (2020) 1–14. https://doi.org/10.1371/journal.pone.0232493.

[30] E.R. Barnea, D. Kirk, S. Ramu, B. Rivnay, R. Roussev, M.J. Paidas, PreImplantation Factor (PIF) orchestrates systemic antiinflammatory response by immune cells: Effect on peripheral blood mononuclear cells, Am J Obstet Gynecol 207 (2012) 1–10. https://doi.org/10.1016/j.ajog.2012.07.017.

[31] T. Wang, B. Ma, G. Hao, Z. Ding, P. Liu, Y. Zhang, J. Liu, Temperature-sensitive hydrogel loaded with minocycline hydrochloride complex for accelerating infected wound healing, J Drug Deliv Sci Technol 88 (2023) 1–13. https://doi.org/10.1016/j.jddst.2023.104961.

[32] F.A. Ngwabebhoh, O. Zandraa, R. Patwa, N. Saha, Z. Capáková, P. Saha, Self-crosslinked chitosan/dialdehyde xanthan gum blended hypromellose hydrogel for the controlled delivery of ampicillin, minocycline and rifampicin, Int J Biol Macromol 167 (2021) 1468–1478. https://doi.org/10.1016/j.ijbiomac.2020.11.100.

[33] A.M. Mueller, B.H. Yoon, S.A. Sadiq, Inhibition of hyaluronan synthesis protects against central nervous system (CNS) autoimmunity and increases CXCL12 expression in the inflamed CNS, Journal of Biological Chemistry 289 (2014) 22888–22899. https://doi.org/10.1074/jbc.M114.559583.

[34] J. Zhao, Y. Wei, J. Xiong, H. Liu, G. Lv, J. Zhao, H. He, J. Gou, T. Yin, X. Tang, Y. Zhang, A multiple controlled-release hydrophilicity minocycline hydrochloride delivery system for the efficient treatment of periodontitis, Int J Pharm 636 (2023) 1–15. https://doi.org/10.1016/j.ijpharm.2023.122802.

[35] M. Müller, Sizing, shaping and pharmaceutical applications of polyelectrolyte complex nanoparticles, Advances in Polymer Science 256 (2014) 197–260. https://doi.org/10.1007/12_2012_170.

[36] Z. Zhang, Z. Wang, J. Nong, C.A. Nix, H.F. Ji, Y. Zhong, Metal ion-assisted self-assembly of complexes for controlled and sustained release of minocycline for biomedical applications, Biofabrication 7 (2015) 1–11. https://doi.org/10.1088/1758-5090/7/1/015006.

[37] V.S. Meka, M.K.G. Sing, M.R. Pichika, S.R. Nali, V.R.M. Kolapalli, P. Kesharwani, A comprehensive review on polyelectrolyte complexes, Drug Discov Today 22 (2017) 1697–1706. https://doi.org/10.1016/j.drudis.2017.06.008.

[38] K. Achazi, R. Haag, M. Ballauff, J. Dernedde, J.N. Kizhakkedathu, D. Maysinger, G. Multhaup, Understanding the Interaction of Polyelectrolyte Architectures with Proteins and Biosystems, Angewandte Chemie - International Edition 60 (2021) 3882–3904. https://doi.org/10.1002/anie.202006457.

[39] R. Buffa, P. Šedová, I. Basarabová, M. Moravcová, L. Wolfová, T. Bobula, V. Velebný, α,β-Unsaturated aldehyde of hyaluronan - Synthesis, analysis and applications, Carbohydr Polym 134 (2015) 293–299. https://doi.org/10.1016/j.carbpol.2015.07.084.

[40] T. Bobula, R. Buffa, P. Procházková, H. Vágnerová, V. Moravcová, R. Šuláková, O. Židek, V. Velebný, One-pot synthesis of α,β-unsaturated polyaldehyde of chondroitin sulfate, Carbohydr Polym 136 (2016) 1002–1009. https://doi.org/10.1016/j.carbpol.2015.10.005.

[41] P. Šedová, R. Buffa, S. Kettou, G. Huerta-Angeles, M. Hermannová, V. Leierová, D. Šmejkalová, M. Moravcová, V. Velebný, Preparation of hyaluronan polyaldehyde - A precursor of biopolymer conjugates, Carbohydr Res 371 (2013) 8–15. https://doi.org/10.1016/j.carres.2013.01.025.

[42] N.A. Peppas, P. Bures, W. Leobandung, H. Ichikawa, Hydrogels in pharmaceutical formulations, European Journal of Pharmaceutics and Biopharmaceutics 50 (2000) 27–46. https://doi.org/https://doi.org/10.1016/S0939-6411(00)00090-4.

[43] R.W. Korsmeyer, R. Gurny, E. Doelker, P. Buri, N.A. Peppas, Mechanisms of solute release from porous hydrophilic polymers, Int J Pharm 15 (1983) 25–35. https://doi.org/https://doi.org/10.1016/0378-5173(83)90064-9.

[44] P. Šedová, R. Buffa, T. Kočí, L. Kovářová, J. Bednařík, H. Vágnerová, V. Velebný, The effect of aminooxy-linkers' structure on the mechanical properties of hyaluronan-oxime hydrogels, Express Polym Lett 16 (2022) 265–278. https://doi.org/10.3144/EXPRESSPOLYMLETT.2022.21.

[45] J.H. Campbell, T.H. Burdo, P. Autissier, J.P. Bombardier, S. V. Westmoreland, C. Soulas, R.G. González, E.M. Ratai, K.C. Williams, Minocycline inhibition of monocyte activation correlates with neuronal protection in SIV NeuroAIDS, PLoS One 6 (2011) 1–11. https://doi.org/10.1371/journal.pone.0018688.

[46] T. Pang, J. Wang, J. Benicky, J.M. Saavedra, Minocycline ameliorates LPS-induced inflammation in human monocytes by novel mechanisms including LOX-1, Nur77 and LITAF inhibition, Biochim Biophys Acta Gen Subj 1820 (2012) 503–510. https://doi.org/10.1016/j.bbagen.2012.01.011.

[47] Y.C. Chen, J. Rivera, M. Fitzgerald, C. Hausding, Y.L. Ying, X. Wang, K. Todorova, S. Hayrabedyan, E.R. Barnea, K. Peter, Preimplantation factor prevents atherosclerosis via its immunomodulatory effects without affecting serum lipids, Thromb Haemost 115 (2016) 1010–1024. https://doi.org/10.1160/TH15-08-0640.

[48] E. Toropitsyn, I. Ščigalková, M. Pravda, V. Velebný, Injectable Hyaluronic Acid Hydrogel Containing Platelet Derivatives for Synovial Fluid Viscosupplementation and Growth Factors Delivery, Macromol Biosci 23 (2023) 1–14. https://doi.org/10.1002/mabi.202200516.

[49] E. Toropitsyn, I. Ščigalková, M. Pravda, J. Toropitsyna, V. Velebný, Enzymatically cross-linked hyaluronic acid hydrogels as in situ forming carriers of platelet-rich plasma: Mechanical properties and bioactivity levels evaluation, J Mech Behav Biomed Mater 143 (2023) 1–12. https://doi.org/10.1016/j.jmbbm.2023.105916.

[50] J.M. Alonso, J.A. Del Olmo, R.P. Gonzalez, V. Saez-martinez, Injectable hydrogels: From laboratory to industrialization, Polymers (Basel) 13 (2021) 1–24. https://doi.org/10.3390/polym13040650.

[51] N. Bhardwaj, S.C. Kundu, Silk fibroin protein and chitosan polyelectrolyte complex porous scaffolds for tissue engineering applications, Carbohydr Polym 85 (2011) 325–333. https://doi.org/10.1016/j.carbpol.2011.02.027.

[52] J. Gummel, F. Cousin, F. Boué, Counterions release from electrostatic complexes of polyelectrolytes and proteins of opposite charge: A direct measurement, J Am Chem Soc 129 (2007) 5806–5807. https://doi.org/10.1021/ja070414t.

[53] Y. Xue, H. Chen, C. Xu, D. Yu, H. Xu, Y. Hu, Synthesis of hyaluronic acid hydrogels by crosslinking the mixture of high-molecular-weight hyaluronic acid and low-molecular-weight hyaluronic acid with 1,4-butanediol diglycidyl ether, RSC Adv 10 (2020) 7206–7213. https://doi.org/10.1039/c9ra09271d.

[54] B. Niemczyk, P. Sajkiewicz, D. Kolbuk, Injectable hydrogels as novel materials for central nervous system regeneration, J Neural Eng 15 (2018) 1–15. https://doi.org/10.1088/1741-2552/aacbab.

[55] U. Ijaz, M. Sohail, M.U. Minhas, S. Khan, Z. Hussain, M. Kazi, S.A. Shah, A. Mahmood, M. Maniruzzaman, Biofunctional Hyaluronic Acid/κ-Carrageenan Injectable Hydrogels for Improved Drug Delivery and Wound Healing, Polymers (Basel) 14 (2022) 1–20. https://doi.org/10.3390/polym14030376.

[56] F. Zhang, S. Zhang, R. Lin, S. Cui, X. Jing, S. Coseri, Injectable multifunctional carboxymethyl chitosan/hyaluronic acid hydrogel for drug delivery systems, Int J Biol Macromol 249 (2023) 1–14. https://doi.org/10.1016/j.ijbiomac.2023.125801.

[57] M. Hu, J. Yang, J. Xu, Structural and biological investigation of chitosan/hyaluronic acid with silanized-hydroxypropyl methylcellulose as an injectable reinforced interpenetrating network hydrogel for cartilage tissue engineering, Drug Deliv 28 (2021) 607–619. https://doi.org/10.1080/10717544.2021.1895906.

[58] L.A. Visser, M. De Mul, W.K. Redekop, Innovative medical technology and the treatment decision-making process in multiple sclerosis: A focus group study to examine patient perspectives, Patient Prefer Adherence 15 (2021) 927–937. https://doi.org/10.2147/PPA.S306132.

[59] L.A. Visser, S.P.I. Huls, C.A. Uyl-de Groot, E.W. de Bekker-Grob, W.K. Redekop, An implantable device to treat multiple sclerosis: A discrete choice experiment on patient preferences in three European countries, J Neurol Sci 428 (2021) 1–11. https://doi.org/10.1016/j.jns.2021.117587.

[60] S.L. Hauser, B.A.C. Cree, Treatment of Multiple Sclerosis: A Review, American Journal of Medicine 133 (2020) 1380–1390. https://doi.org/10.1016/j.amjmed.2020.05.049.

LIST OF FIGURES

FIG. 1.1: RISK OF SYSTEMIC ADMINISTRATION ROUTE OF THE DISEASE MODIFYING THERAPIES..... 11

FIG. 1.2: MINOCYCLINE STRUCTURE: A) METAL ION CHELATION SITES, B) CHELATION STRUCTURE OF MN WITH CALCIUM (HOLMKVIST ET AL., 2016; Z. ZHANG ET AL., 2015). 12

FIG. 1.3: STRUCTURE OF SYNTHETIC PREIMPLANTATION (SPIF)..... 12

FIG. 2.1: OVERVIEW OF THE THESIS OBJECTIVES. STEP 1) MATERIALS SELECTION AND ENTRAPMENT STRATEGY FOR DELIVERING REPURPOSED DMTS. THE PURPLE SPHERE REPRESENTS THE CONVENTIONAL NANOPARTICLE-BASED DRUG ENTRAPMENT APPROACH, WHILE THE ORANGE SPHERE ILLUSTRATES THE PROPOSED METHOD, WHERE THE DRUG IS ENCAPSULATED IN A PEC IMMOBILIZED WITHING THE HAOX-CSOX HYDROGEL STRUCTURE. STEP 2) CHARACTERIZATION OF DDS. STEP 3) IN VITRO BIOACTIVITY TESTING TO EVALUATE THE COMPATIBILITY OF THE DDS WITH THE ENCAPSULATED DMTS. 14

FIG. 3.1: SCHEMATIC OF A PAIR-SYRINGE SYSTEM CONNECTED BY A LUER LOCK ADAPTER OR MIXING PORT USED IN THE CROSSLINKING PROCESS OF HAOX AND HAOX-CSOX HYDROGEL. 16

FIG. 3.2: ILLUSTRATION OF TRANSWELL® SYSTEM. A POROUS MEMBRANE SEPARATES TWO CHAMBERS, WITH DMTS-LOADED DDS INTRODUCED IN THE UPPER COMPARTMENT AND DRUG RELEASE IS QUANTIFIED IN THE LOWER COMPARTMENT. 19

FIG. 4.1: ^{1}H NMR OF ALDEHYDE MODIFIED CHONDROITIN SULFATE. 21

FIG. 4.2: COMPARATIVE ASSESSMENT OF GELATION PROFILE FOR HYDROGELS BASED ON CSOX, HAOX, AND PEC (UNBOUND AND IMMOBILIZED). RESULT FROM TRIPLICATE TRIALS (N =3) SHOW **** $P < 0.0001$ FOR CSOX-MN VERSUS PURE HAOX). 22

FIG. 4.3: SUSTAINED AND BURST-RELEASE PATTERNS OF MINOCYCLINE FROM DDS: SUBFIGURE (A) ILLUSTRATES TIME-DEPENDENT CDR FOR HAOX-CSOX HYDROGELS; SUBFIGURE (B) QUANTIFIES BURST-RELEASE. STATISTICAL ANALYSIS (N=3): ** $P < 0.01$, *** $P < 0.001$, NS IS NON-SIGNIFICANT. 23

FIG. 4.4:QUANTITATIVE SWELLING PROFILE OF DDS FORMULATIONS (SWELLING RATIO VS. TIME; N=3). 24

FIG. 4.5: GELATION TIME OF INJECTABLE HYDROGELS CONTAINING FITC-SPIF, MEASURED AT TWO PREPARATION PH VALUES (5.0 AND 6.8). EACH GROUP INCLUDES THREE FORMULATIONS WITH INCREASING CSOX CONCENTRATIONS: NO CSOX (HAOX_15 AT PH 5, HAOX_17 AT PH 6.8), 0.5% CSOX (HACOX_25, HACOX_27), AND 1% CSOX (HACOX_35, HACOX_37). RESULTS REPRESENT MEAN ± SD (N = 3). 25

FIG. 4.6: DRUG RELEASE PROFILE ACROSS DIFFERENT PREPARATION PH AND FORMULATION, A) CUMULATIVE DRUG RELEASE, B) BURST PROFILE, C) T50%. DATA ARE EXPRESSED AS MEAN ± SD (N = 3). SIGNIFICANCE LEVELS: *$P < 0.05$, **$P < 0.01$, ***$P < 0.001$, ****$P < 0.0001$, NS = NON-SIGNIFICANT. 26

FIG. 4.7: SWELLING RATIO OF FORMULATION PREPARED AT PH 6.8 (N=3). 27

FIG. 4.8: TGF-β EXPRESSION AFTER TREATMENT WITH FITC-SPIF. 28

LIST OF TABLES

TABLE 1.1 FDA APPROVED DISEASE MODIFYING THERAPIES [3,6–8]. 10

TABLE 3.1 SERIES OF STUDIED FORMULATIONS FOR MN-DDS. 17

TABLE 3.2 FORMULATIONS FOR DESIGNING A SUITABLE DELIVERY SYSTEM FOR SPIF. 18

TABLE 3.3 DEVELOPMENT OF HACOX_37: INFLUENCE OF FITC-SPIF LOADING LEVELS ON CDR, SWELLING BEHAVIOUR, AND KORSMEYER-PEPPAS MODELLING. 18

TABLE 3.4 DEVELOPMENT OF HACOX_37: INFLUENCE OF CSOX CONCENTRATION ON CDR, SWELLING BEHAVIOUR, AND KORSMEYER-PEPPAS MODELLING. 18

TABLE 4.1 INJECTABILITY ASSESSMENT OF HAOX_PECOX FORMULATION USING DYNAMIC GLIDE FORCE (DGF) AND MAXIMUM FORCE (FMAX) METRICS (N=3). 22

TABLE 4.2 KORSMEYER-PEPPAS RELEASE FITTING ACROSS FORMULATIONS. 23

TABLE 4.3 KORSMEYER-PEPPAS KINETIC MODELLING OF FITC-SPIF RELEASE FROM DDS PREPARED AT VARIED PH LEVELS (N=3). 27

TABLE 4.4 INJECTABILITY PARAMETERS OF HACOX_37, EVALUATED THROUGH DYNAMIC GLIDE FORCE (DGF) AND MAXIMUM EXTRUSION FORCE (FMAX) (N=3). 28

LIST OF ABBREVIATIONS

BBB	Blood-Brain Barrier
CA	Calcium Chloride
CDR	Cumulative Drug Release
CIS	Clinically Isolated Syndrome
CNS	Central Nervous System
CS	Chondroitin Sulfate
CSF	Cerebrospinal Fluid
CSOX	Aldehyde-modified chondroitin sulfate
DDS	Drug Delivery Systems
DF	Degree of Functionalization
DGF	Dynamic Glide Force
DMT	Disease-Modifying Therapies
ELISA	Enzyme-Linked Immunosorbent Assay
FDA	Food and Drug Administration
FITC-SPIF	Fluorescein isothiocyanate–modified Synthetic Preimplantation Factor

GA	Gelatine type A
GalNAc	N-acetylgalactosamine
HA	Hyaluronic acid
HAOX	Aldehyde-modified hyaluronic acid
IFN-	Interferon
IL-	Interleukin
LPS	Lipopolysaccharide
MN	Minocycline
MS	Multiple sclerosis
PDHA	Propanediylbishydroxylamine Dihydrochloride
PDLLA-PEG-PDLLA	Poly(D,L-lactide)-block-poly(ethylene glycol)-block-poly(D,L-lactide)
PECs	Polyelectrolyte Complexes
PMA	Phorbol 12-yristate 13-acetate
PPMS	Primary Progressive Multiple Sclerosis
qRT-PCR	quantitative Reverse Transcription Polymerase Chain Reaction
RRMS	Relapsing-Remitting Multiple Sclerosis
SEC-MALLS	Size-exclusion chromatography and multi-angle laser light scattering
SPIF	Synthetic Preimplantation Factor
SPMS	Secondary Progressive Multiple Sclerosis
TGF-	Transforming growth factor
U.S.	United States
WB-MAT	Whole Blood Monocytes Activation Test

CURRICULUM VITAE

Personal Information

Name	Tutut Ummul Habibah
Address	Dukelska 546/604, Ustí nad Orlici, Czech Rep.
Telephone	+420 773 032 919
Email	habibah@utb.cz / habibahtutut@gmail.com
Nationality	Indonesian
Date of birth	09. 08. 1992

Education and Training

Dates	2021 – present
Title of qualification	Doctoral study – expected defence 2025
Principal Branch	Technology of Macromolecular Substances
School	Faculty of Technology – Tomas Bata University in Zlin

Dates	2015 – 2016
Title of qualification	M.Sc.
Principal Branch	Biomaterials Science
School	School of Materials – The University of Manchester, UK

Dates	2011 – 2015
Title of qualification	B.Eng.
Principal Branch	Technology of Materials and Metallurgy
School	Materials and Metallurgy – Sepuluh Nopember Institute of Technology, Indonesia

LIST OF PUBLICATION

1. **T. Habibah**, J. Matonohová, J. Kulhánek, U. Fitzgerald, M. Ingr, M. Pravda, A. Pandit, V. Velebný, In situ formed aldehyde-modified hyaluronic acid hydrogel with polyelectrolyte complexes of aldehyde-modified chondroitin sulfate and gelatin: An approach for minocycline delivery, Carbohydr Polym 343 (2024). https://doi.org/10.1016/j.carbpol.2024.122455.

2. **T. Habibah**, A. Exnerová, K. Nešporová, U. FitzGerald, A. Pandit, M. Ingr, M. Pravda, V. Velebný, In situ delivery of synthetic preimplantation factor using aldehyde-modified hyaluronic acid hydrogel with immobilized complexes of chondroitin sulfate derivatives, Carbohydrate Polymer Technologies and Applications 9 (2025). https://doi.org/10.1016/j.carpta.2025.100689.

OVERVIEW OF OTHER ACTIVITIES

Conference:

T. Habibah, M. Ingr, M. Pravda. (2023), Polyelectrolyte Complex-loaded Hyaluronic Acid Hydrogel for Minocycline Release. DGM FEMS EUROMAT 2023 (Materials Science and Technology in Europe), Frankfurt am Main.

Studies abroad:

One month secondment program for viability study on the influence of release products from the drug-containing hydrogel and drug-containing particles on human oligodendroglial and neuronal cells at Universitätsklinikum Münster, Institut für Neuropathologie, Arbeitsgruppe Prof. Tanja Kuhlmann, WWU MÜNSTER (Germany), October 2022.

Summer schools:

- **In Vitro Model Systems for the Study of Neurodegenerative Disease**, May 25–27, 2021 (Online, South Denmark University)
- **Animal Models in MS Research, Scientific Integrity**, Intellectual Property, and Practical MRI Skills, May 30 – June 3, 2022 (University of Antwerp, Belgium)
- **Hyaluronan Hydrogel and Its Technological Transfer**, November 22–24, 2022 (Contipro a.s., Czech Republic.

Tutut Ummul Habibah, Ph.D

Development and Evaluation of a Multi-Modal Hyaluronic Acid Hydrogel for Anti-Inflammatory Drug Delivery for Multiple Sclerosis Therapy

Vývoj a charakterizace multimodálního hydrogelu kyseliny hyaluronové s řízeným uvolňováním protizánětlivých léčiv k léčbě roztroušené sklerózy

Doctoral Thesis Summary

Published by: Tomas Bata University in Zlín,

nám. T. G. Masaryka 5555, 760 01 Zlín.

Edition: published electronically

Typesetting by: Author

This publication has not undergone any proofreading or editorial review.

Publication year: 2025

First Edition

ISBN 978-80-7678-351-5